Wind and Structures, *Vol. 18, No. 3 (2014) 267-279*
DOI: http://dx.doi.org/10.12989/was.2014.18.3.267

Hydrodynamic response of alternative floating substructures for spar-type offshore wind turbines

Baowei Wang[a], SajadRahmdel[b], Changwan Han, Seungbin Jung and Seonghun Park*

School of Mechanical Engineering, Pusan National University, Busan, Republic of Korea

(Received July 30, 2012, Revised December 9, 2013, Accepted December 15, 2013)

Abstract. Hydrodynamic analyses of classic and truss spar platforms for floating offshore wind turbines (FOWTs) were performed in the frequency domain, by considering coupling effects of the structure and its mooring system. Based on the Morison equation and Diffraction theory, different wave loads over various frequency ranges and underlying hydrodynamic equations were calculated. Then, Response Amplitude Operators (RAOs) of 6 DOF motions were obtained through the coupled hydrodynamic frequency domain analysis of classic and truss spar-type FOWTs. Truss spar platform had better heave motion performance and less weight than classic spar, while the hydrostatic stability did not show much difference between the two spar platforms.

Keywords: floating offshore wind turbines (FOWT); classic spar platform; truss spar platform; frequency domain; hydrostatic analysis; hydrodynamic analysis; finite element method

1. Introduction

Offshore wind energy has become one of the most promising renewable energy resources because of its advantages, such as steadier and stronger wind with less turbulence, lower area cost, less visual and noise pollution (Leung and Yang 2012, Snyder and Kaiser 2009, Tavner 2008). To harness offshore wind energy, different offshore wind turbine concepts are proposed in the literature. (Breton and Moe 2009, Byrne and Houlsby 2003). For shallow waters, fixed platform concepts, such as tripod, jack-ups, and compliant towers are proposed, while for deep waters, floating platform concepts, such as tension-leg, semi-submersible, and spar platforms are proposed (Hua 2011, Moe 2010).

Kurian *et al*. performed both numerical and experimental studiesfor the dynamic responses of classic and truss spar platforms considering random wave and current forces. A 1:100 scale model was usedto carry out the experiment and the dynamic responses were obtained in the frequency domain. By using free decay test, damping ratio and natural periods of the system were obtained. Furthermore, Response Amplitude Operators (RAOs) were calculated for heave, surge, and pitch

∗Corresponding author, Professor, E-mail: paks@pusan.ac.kr
[a] Graduate student, E-mail: wangbw1986@gmail.com
[b] Graduate student, E-mail: rahmdel.s@gmail.com

http://www.techno-press.org/?journal=was&subpage=8 ISSN: 1226-6116 (Print), 1598-6225 (Online)

motions. The experimental results and numerical results had good agreement and it showed that coupled wave and current forces would result in higher surge, heave, and pitch motions for the classic spar compared with the truss spar platform. It was also concluded that the dynamic responses in the surge, heave and pitch of both types of spar platforms increased as the current velocities increased under the same random wave. Moreover, they experimentally investigated the dynamic motions (i.e., RAOs of surge, heave and pitch motions) of classic and truss spar platforms subjected to multi-directional waves and found that multi-directional waves generate smaller dynamic motions in comparison with long crested waves(Kurian *et al.* 2012a, b, Kurian *et al.* 2012).

Robertson and Jonkman studied the dynamic responses of six offshore wind turbine platforms. These platforms were two tension-leg platforms (TLP), a semi-submersible platform, a barge platform, and two spar platforms. Using IEC 61400-3 standard, various load cases were analyzed and the dynamic responses of the platforms were compared with each other. From the comparison, it was concluded that the barge platform has the highest dynamic motion. The TLP, semi-submersible, and spar platforms have almost similar dynamic responses, however, semi-submersible and spar platforms had greater loads in their towers than the barge platform(Robertson and Jonkman 2011).

As for the spar platform, three configurations, namely classic-spar, truss-spar, and cell-spar are used in the oil and gas (O&G) industry (Wilson 2003). According to the study of oil and gas industry, truss-spar platform has lower cost and better performance compared with classic spar (Berthelsen *et al.* 2000). However, only two spar prototypes, namely Hywind and Sway, have been used in offshore wind industry so far (Angela 2008).

Using spar platform for offshore wind turbines is a new concept and a limited number of studies have been carried out in the relevant research community. This study aims to conduct the coupled hydrodynamic analyses of both classic and truss spar platforms for floating offshore wind turbines as well as to comprehensively compare dynamic performances of both spar platforms in the frequency domain. As shown in the literature review above, Kurian *et al*. also did several researches related to this study, however, in their studies, they did not include the effects of wind turbine superstructure on calculating the dynamic motions of the spar platforms. In this study, the effects of superstructure are considered in all hydrodynamic analyses and the dynamic motions of classic and truss spar platforms are compared much more comprehensively than the previous study of Kurian *et al*. (Kurian *et al*. 2012a, b, Kurian *et al*. 2012). Furthermore, the dimensions of the spar platforms and the mooring lines used in this study are based on the state of the art technology used in the Hywind project, which could enhance the hydrodynamic stability of the spar platforms.

2. Methodology

2.1 Structure's configurations

The classic spar hull is assumed to be hermetically sealed (Sarpkaya *et al.* 1981). The truss spar platform hassimilar configuration with the classic spar except that the middle section is replaced with truss elements. In this study the effects of the mooring system are considered by giving specified pretension stiffness on specified loading points on the hull of platforms (Wang *et al.* 2008).

The specifications of the two spar platforms (Fig. 1) are based on (Hywind brochure 2012) with minor modifications.

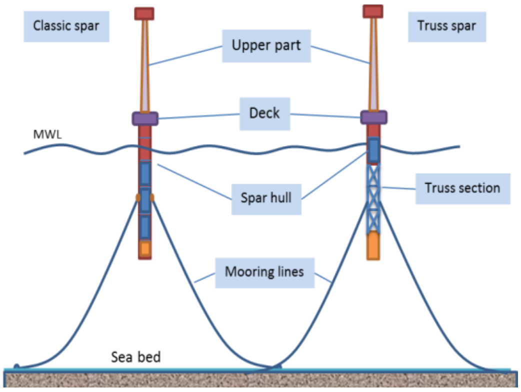

Fig. 1 Classic and truss spar configurations

Table 1 Specifications of the two spar platforms

Items	Classic-spar	Truss-spar
Hull diameter [m]	8	8 (Hull) 0.50 (Pillar) 0.45 (Truss)
Submerged depth (Total draft) [m]	100	100
Actual volumetric displacement [m^3]	4994	3610
Total mass [tons]	4.99e03	3.61e03
Center of gravity (Centerline) [m]	-69	-57
Moment of inertial, I_{xx} [kg.m^2]	1.01e10	9.54e09
Moment of inertial, I_{yy} [kg.m^2]	1.01e10	9.54e09
Moment of inertial, I_{zz} [kg.m^2]	4.40e07	3.36e07
Sea water density [kg/ m^3]	1025	1025

For both spar platforms, the loading conditions (Table 1) are adjusted to be similar to make the comparison reasonable.

2.2 Assumptions

Only wave loads are considered as environmental loads, because wave loads have the most influence on dynamic behaviors of floating platforms. Also, for simplicity, wind and current loads are not considered in analysis. Furthermore, water is assumed to be ideal, non-rotational and incompressible fluid with small wave elevations (Ansys 2009).

2.3 Definition of motions

The spar platforms are anchored to seabed using mooring line system, while the entire structure undergoes rigid body motions in six DOFs (Agarwal and Jain 2003). A right-handed coordinate

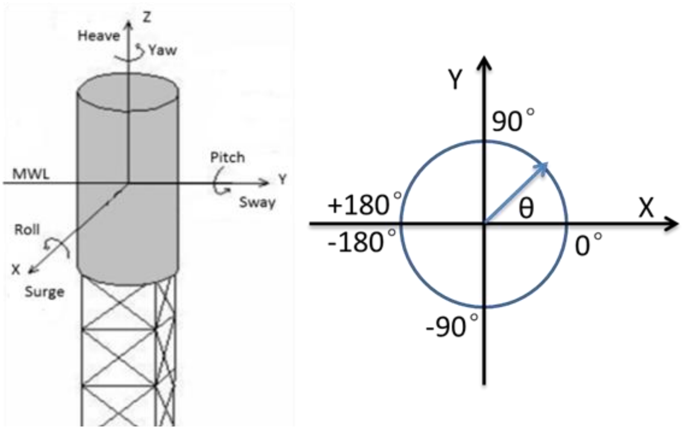

Fig. 2 Definition of motions and wave direction

system with the origin at the mean water level (MWL) is used, and the positive Z axis is set as the vertically upward direction. The system motions are described by six DOFs, where surge, sway and heave are translational motions while roll, pitch and yaw are rotational motions (Fig. 2(a)). The wave direction is calculated as the angle between wave front and positive X axis which is measured anticlockwise (Fig. 2(b)).

2.4 Calculation of wave loads

Linear Diffraction theory is used to calculate the inertia forces and diffraction forces acting on the main bodies of the spar platforms. Also, using Morison equation, wave drag forces acting on the truss section of the truss spar platform are calculated. Furthermore, boundary element method (BEM) is used to solve and discretize coupled motion equations of the spar platforms (Wilson 2003).

The governing equation for velocity potential is

$$\nabla^2 \phi = 0 (\vec{V} = \nabla \phi) \tag{1}$$

Linearized free surface condition becomes

$$\frac{\partial \emptyset}{\partial z} - \frac{\omega^2}{g} \emptyset = 0 \tag{2}$$

where ω is the wave frequency and ϕ is the velocity potential. Seabed boundary conditions are

$\nabla \phi = 0$ when $z \to \infty$ (for deep water)

$\frac{\partial \phi}{\partial z} = 0$ at $z = -d$ (for shallow water)

By the linearized assumption, the velocity potential is decomposed into incident wave velocity potential, diffracted wave velocity potential, and radiated wave potential in the six DOFs. A linear superposition of velocity components is applied to obtain the total velocity potential due to unit amplitude incident wave, and the total velocity potential becomes

$$\phi = \varphi \mathrm{e}^{-i\omega t} = \left[\left(\varphi_I + \varphi_{di} \right) + \sum_{j=1}^{6} \varphi_j \cdot x_j \right] \mathrm{e}^{-i\omega t} \tag{3}$$

where *I* is the velocity potential for incident wave, *di* is the diffracted wave, and j = 1,2,…6 is the radiated wave in six DOFs. x_j is the structure motion for the unit wave amplitude. The incident wave velocity potential for finite water depth *d*, is defined as follows

$$\varphi_I \mathrm{e}^{-i\omega t} = \frac{-ig\zeta \cosh\left[k\left(z+d \right) \right] \mathrm{e}^{ik\left(x\cos\theta + y\sin\theta + \alpha \right)} \mathrm{e}^{-i\omega t}}{\omega \cosh\left(kd \right)} \tag{4}$$

where d is the water depth, θ is the wave direction, ζ is the wave elevation, and k is the wave number defined by

$$\omega^2 = gk \tanh(kd) \tag{5}$$

After the velocity potentials of the incident and diffracted wave are determined, the hydrodynamic pressure acting on the surface of the structure could be calculated using the Bernoulli equation as follows (Wilson 2003)

$$P = -\rho \frac{\partial \phi}{\partial t} \tag{6}$$

where P is the hydrodynamic pressure and ρ is the water density. The various fluid forces could be calculated by integrating the hydrodynamic pressure over the wetted surface of the body. For Morison structures (D/λ < 0.2), the wave force could be calculated using Morison equation as follows

$$\boldsymbol{F} = \rho \Omega \boldsymbol{a}_w + \rho C_a \Omega \boldsymbol{a}_w - \rho C_a \Omega \ddot{\boldsymbol{X}} + \frac{1}{2} \rho C_d D \boldsymbol{V} \left| \boldsymbol{V} \right| \tag{7}$$

where C_a and C_d are the added mass and drag coefficients of the element, respectively (Wilson 2003). Ω *is* the volume of the element per unit length, D is the element diameter, $\boldsymbol{a_w}$ is the instantaneous flow acceleration, V is the relative velocity between the flow and structure, and $\ddot{\boldsymbol{X}}$ is the structure acceleration due to oscillation.

2.5 Wave frequency motions

The external loads acting on the spar platforms could be calculated if the velocity potentials of the incident, diffracted wave, and radiated wave are available. Also, the added mass and added damping could be calculated based on diffraction theory. In general, the linear coupled equation of motion is written using the following matrix form (Berthelsen *et al.* 2000)

$$\left(\boldsymbol{M}_s + \boldsymbol{M}_a \right) \ddot{\boldsymbol{X}} + \boldsymbol{C}\dot{\boldsymbol{X}} + \boldsymbol{K}\boldsymbol{X} = \boldsymbol{F}_0 \mathrm{e}^{-i\omega t} \tag{8}$$

where $\boldsymbol{M_S}$ is the mass matrix of the structure, $\boldsymbol{M_a}$ is the added mass (6×6 matrix) by frequency, $\boldsymbol{C}$ is the linear damping matrix (6×6 matrix), $\boldsymbol{K}$ is the restoring stiffness matrix (6×6 matrix), and $\boldsymbol{F_0}$ is the total external force. The solution was assumed to be harmonic by

$$\boldsymbol{X} = \boldsymbol{X}_0 \mathrm{e}^{-i\omega t} \tag{9}$$

where $\boldsymbol{X_0}$ is the complex amplitude vector. Substituting Eq. (9) into Eq. (8) yields the following

$$\left[-\omega^2\left(\boldsymbol{M_s}+\boldsymbol{M_a}(\omega)\right)-i\omega\boldsymbol{C}(\omega)+\boldsymbol{K}\right]\boldsymbol{X}_{(\omega)} = \boldsymbol{F}_0\mathrm{e}^{-i\omega t} \tag{10}$$

and the solution has the following form

$$\boldsymbol{X}_0 = \left[-\omega^2\left(\boldsymbol{M_S}+\boldsymbol{M_a}(\omega)\right)-i\omega\boldsymbol{C}(\omega)+\boldsymbol{K}\right]^{-1}\boldsymbol{F}_0 \tag{11}$$

Response amplitudes are given in complex notation as follows

$$\boldsymbol{X}_0 = \begin{bmatrix} X_1 \\ X_2 \\ \vdots \\ X_3 \end{bmatrix} = \begin{bmatrix} X_1^{Re} + iX_1^{Im} \\ X_2^{Re} + iX_2^{Im} \\ \vdots \\ X_n^{Re} + iX_n^{Im} \end{bmatrix} \tag{12}$$

where the magnitude is

$$|X_i| = \sqrt{\left(X_i^{Re}\right)^2 + \left(X_i^{Im}\right)^2} \tag{13}$$

The response amplitude operator (RAO) is defined as the response divided by the wave amplitude

$$\mathrm{RAO_i} = \left|\frac{x_i}{\frac{1}{2}H_w}\right| = \left|\frac{\sqrt{\left(X_i^{Re}\right)^2 + \left(X_i^{Im}\right)^2}}{\frac{1}{2}H_w}\right| \tag{14}$$

where $\frac{1}{2}H_w$ is the wave amplitude. The irregular wave is described using JONSWAP wave spectrum (Fig. 3).

In hydrodynamic response analysis, RAOs are normally used to evaluate the performance of the structure in the frequency domain. Fig. 4 summarizes process for determining the calculation-related terms in Eq. (11).

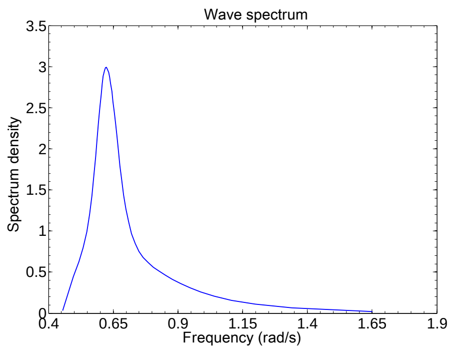

Fig. 3 Wave spectrum in simulation

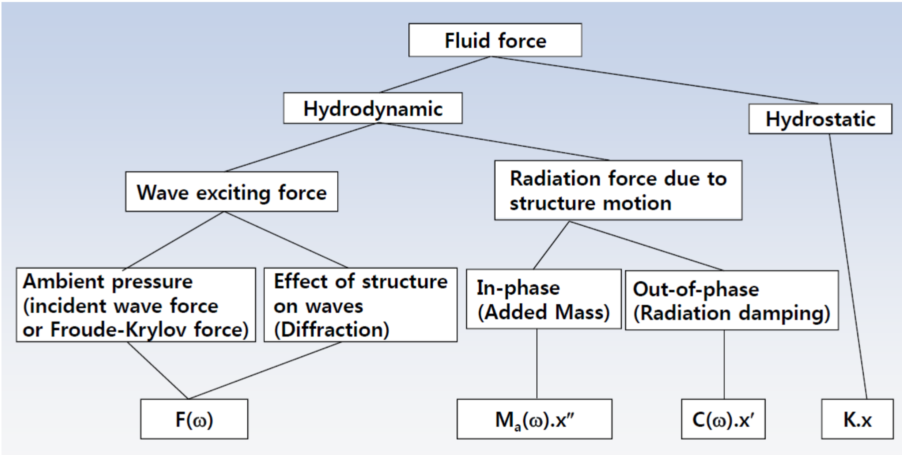

Fig. 4 The process of wave force calculation in ANSYS AQWA^{TM}

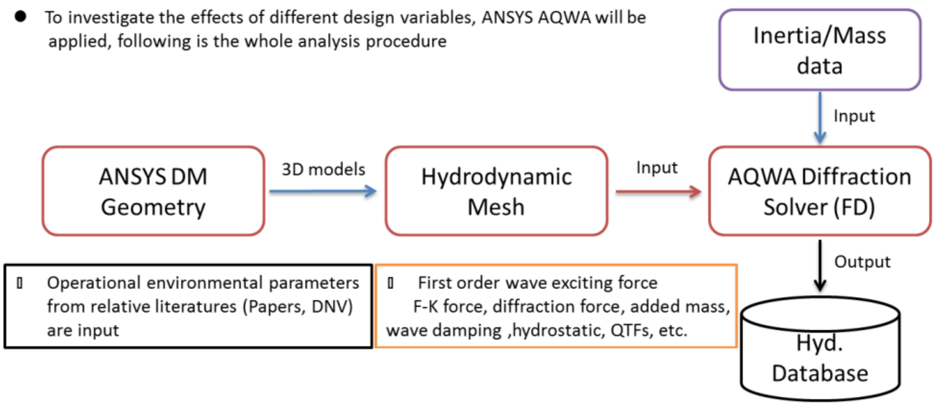

Fig. 5 Procedure of dynamic behavior analysis

2.6 Analysis procedure

ANSYS AQWA software package was used to carry out dynamic analysis. This software package has a diffraction analysis solver in the frequency domain (FD) named AQWA-LINE. ANSYS AQWA was used to obtain the hydrostatic loads, first order wave exciting forces, and quadratic transfer functions (QTFs) for the calculation of slowly varying wave drift forces (Fig. 5).

The finite element method (FEM) was applied to predict the hydrodynamic response using ANSYS AQWA^{TM} software. Fig. 6 shows the finite element model created in ANSYS.

Both spar platforms were symmetric about the x and y axis. The incident wave angle was chosen from 0 to 180° with an interval of 45°. The RAOs of 0°, 45° and 90° for classic and truss spar platforms were determined in the wave frequency ranged from 0 rad/s to 2.5 rad/s. Then, the RAOs in the different DOFs and wave directions were obtained from the simulation results.

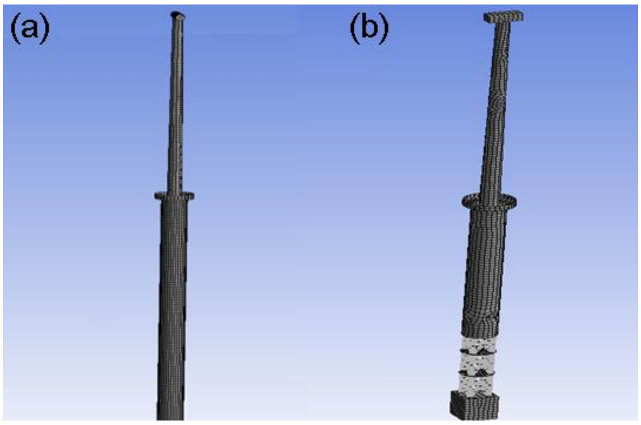

Fig. 6 Finite element models (surface elements) of (a) classic spar and (b) truss spar

3. Results and discussion

3.1 Hydrostatic results

External loads such as waves try to turn the floating structure over, while the structure must be able to resist these loads through what is termed as hydrostatic stability. Table 2 lists the hydrostatic results for the spar platforms. Metacentric heights are the key parameters needed to evaluate the stability of the two spar platforms and as listed in the table, both metacentric heights of the spars were positive and similar (a positive metacentric height makes the structure stable) (Kampf 2009).

3.2 Frequency domain analysis of RAOs

RAOs for chosen incident wave directions are shown in Figs. 7-8, however, RAOs of some directions were not included because they had insignificant impacts on the structure's motions.

Table 2 Hydrostatic properties of the spar platforms

Specifications	Classic spar	Truss spar
Center of Buoyancy (Centerline) [m]	-50	-41.6
Cutter water area [m²]	49.5	49.5
Center of gravity to center of buoyancy [m]	-19	-15
Metacentric Heights, GMX [m]	19	15.5
Metacentric Heights, GMY [m]	19	15.5

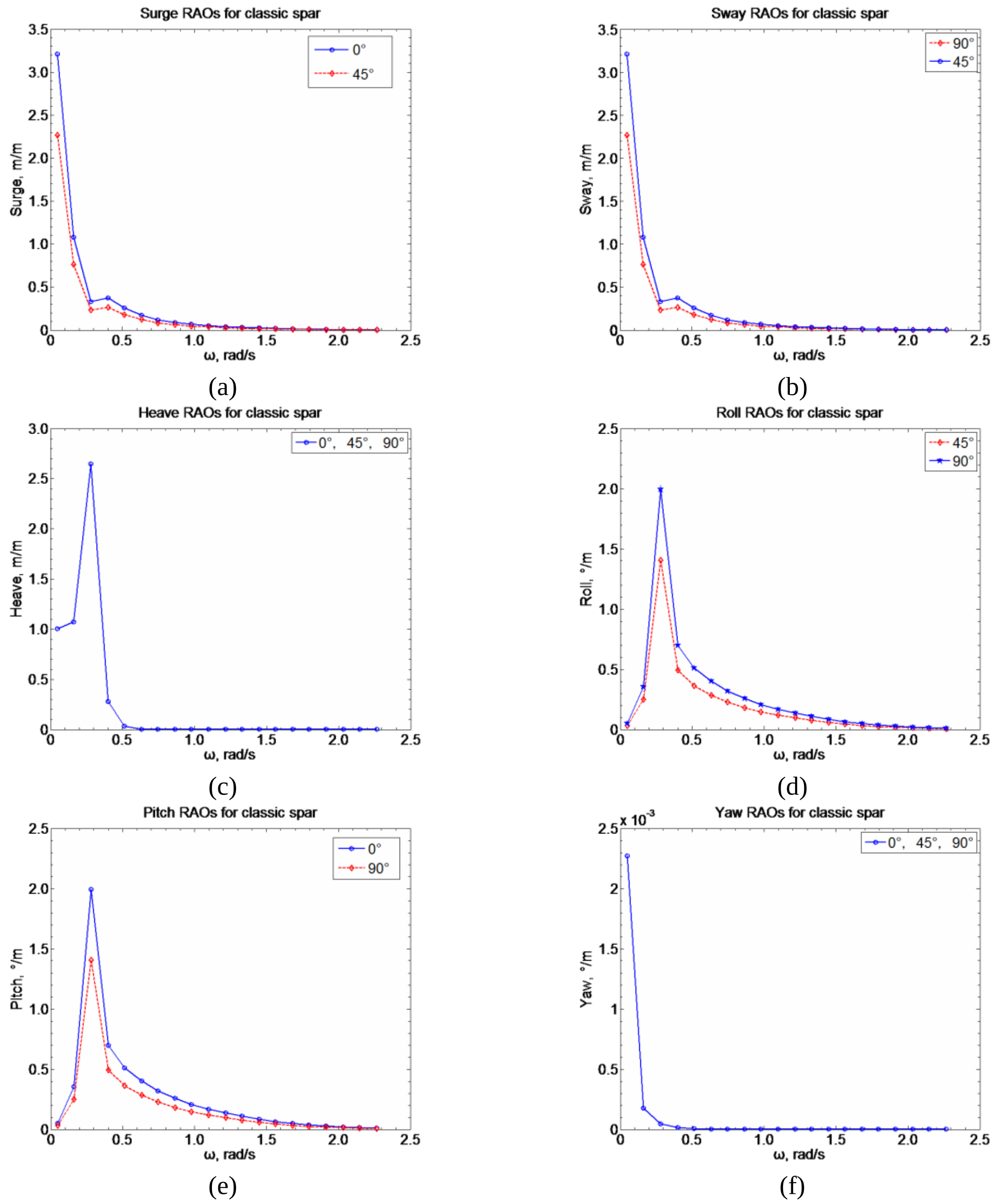

Fig. 7 Response amplitude operators (RAOs) of classic spar platform for (a) surge motion, (b) sway motion, (c) heave motion, (d) roll motion, (e) pitch motion, and (f) yaw motion

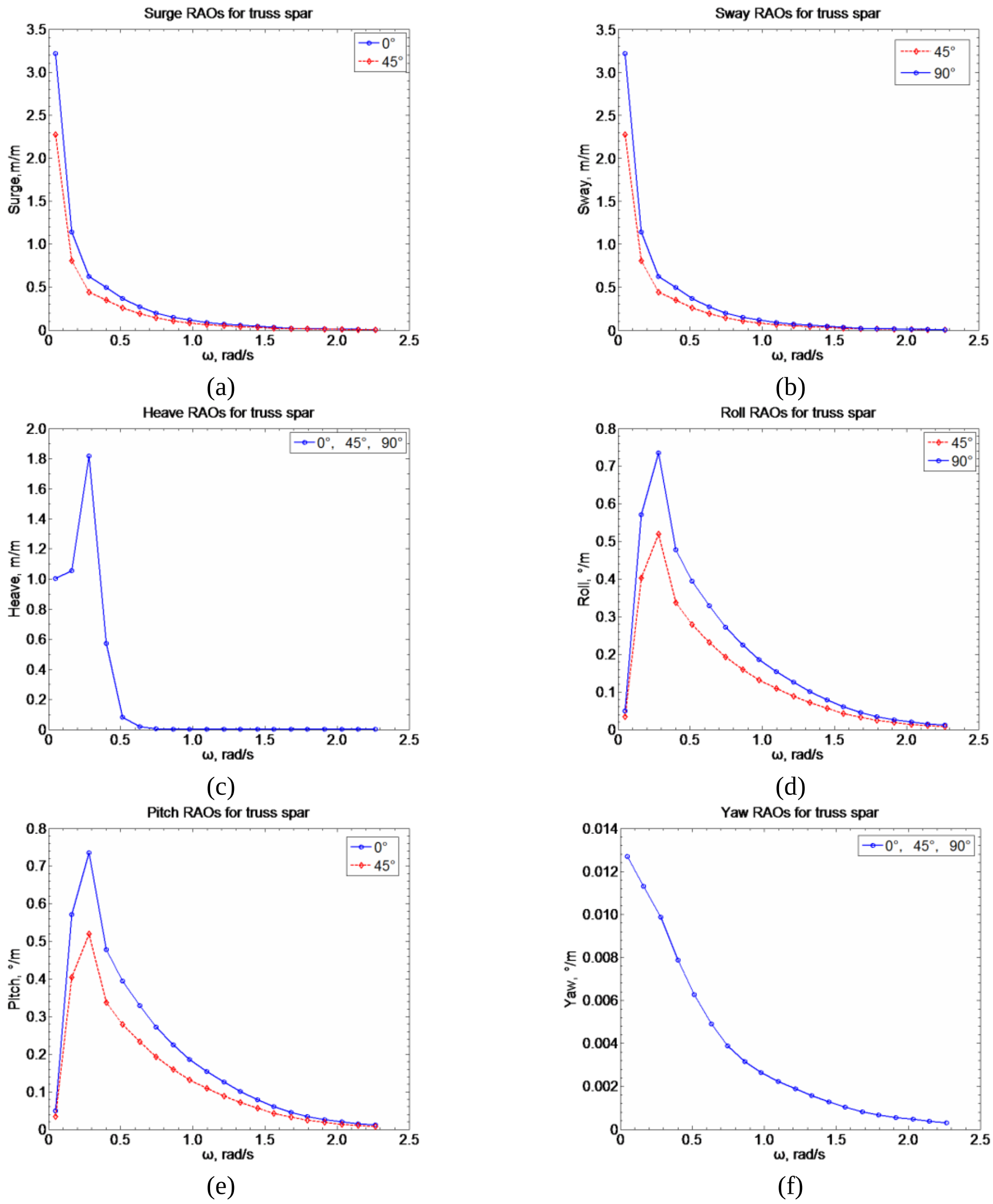

Fig. 8 Response amplitude operators (RAOs) of truss spar platform for (a) surge motion, (b) sway motion, (c) heave motion, (d) roll motion, (e) pitch motion, and (f) yaw motion

From Figs. 7(a) and 8(a), it was observed that the magnitudes of surge and sway motions of both spar platforms were similar to each other. There was only one single curve in the graph of the heave RAOs, which is because the heave motion is independent of the incident wave angle for both spar platforms. As shown in Figs. 7(c) and 8(c), the maximum heave RAO of the classic spar is much larger than that of the truss spar, which means that replacing the middle section of the classic spar withtruss elements improves the heave response of the structure. Truss spar has less heave, roll and pitch motions compared with classic spar platform (Figs. 7(c) - 7(e)) and Figs. 8(c) - (e), suggesting that truss spar has better stability. The yaw motions of both platforms were negligible and approximately zero at all incident wave angles and frequencies examined. For both spar platforms, the roll and pitch were symmetrical with regard to the incident wave angle, like the surge and sway. In addition, the magnitudes of the roll and pitch for the truss spar were smaller than those of the classic spar platform.

By using the results of this study, comprehensive comparisons between dynamic motions of classic and truss spar platforms are described in Table 3.

Table 3 Comparisons between dynamic motions of classic and truss spar platforms

	Classic Spar	Truss Spar	Discussion
Structure weight	4.99e3	3.61e3	The total mass of the truss spar platform is less compared with the classic spar, which indicates truss spar has less fabrication and production costs.
Highest surge motion (m)	3.21	3.21	Both spars have the same surge motions
Highest sway motion (m)	3.21	3.21	Both spars have the same sway motions
Highest heave motion (m)	2.65	1.82	The heave motion of truss spar platform is smallerthanthat of classic spar, because, in truss spar, heave plates reduce the heave motion of the structure.
Highest roll motion (degree)	1.99	0.74	The highest roll and pitch motions of truss spar platform are smaller compared with classic spar. However, the highest roll motion is the same as the highest pitch motion due to the same wave incident angle (0^o) inboth roll and pitch directions, which creates the same wave loads in these directions.
Highest pitch motion (degree)	1.99	0.74	
Highest yaw motion (degree)	2.27e-03	4.06e-02	Yaw motions of both spar platforms are small and negligible.

4. Conclusions

Coupled hydrodynamic analysis of two different types of spar platforms, namely classic spar and truss spar, were conducted in the frequency domain. It was found that truss spar platform had better heave motion performance than classic spar, although the hydrostatic stability of both spar platforms was similar to each other. These results suggest that truss spar had higher total stability compared with classic spar platform. It was also found that truss spar platform had less weight (i.e., less fabrication materials and cost), indicating that truss spar was more economical than classic spar.

In this study, only wave loads were taken into account, however, in future studies, coupled wind, current, and wave loads would be considered as environmental loads. To include all these loads, time domain analyses are required which will be conducted using a hydrodynamic time response software package. Moreover, the effects of wind turbine motions on spar platforms will be considered to produce more accurate results on the dynamic behavior of spar-type platforms.

Acknowledgments

This work was supported by the Human Resources Development program (No. 20113020020010-11-1-000) of the Korea Institute of Energy Technology Evaluation and Planning (KETEP) grant funded by the Korea government Ministry of Trade, Industry and Energy and by Leading Foreign Research Institute Recruitment Program through the National Research Foundation of Korea (NRF) funded by the Ministry of Science, ICT & Future Planning (No.2013044133).

References

Agarwal, A. and Jain, A. (2003), "Dynamic behavior of offshore spar platforms under regular sea waves", *Ocean Eng.*, **30**(4), 487-516.

Angela, N. (2008), "StatoilHydro to pilot test first offshore floating wind turbine", *Power*, **152**(7), 13-14.

Ansys. (2009). *ANSYS AQWATM-line manual release 12.0*, Retrieved from http://orange.engr.ucdavis.edu/ Documentation12.1/121/AQWA/aqwa-line.pdf .

Berthelsen, P.A., Incecik, A. and Downie, M.J. (2000), *Dynamic response analysis of a truss spar in waves*, Master degree thesis, University of Newcastle.

Breton, S.P. and Moe, G. (2009), "Status, plans and technologies for offshore wind turbines in Europe and North America", *Renew. Energ.*, **34**(3), 646-654.

Byrne, B. and Houlsby, G. (2003), "Foundations for offshore wind turbines", *P. Roy. Soc. London. A – Math. Phy.*, **361**(1813), 2909-2930.

Hua, J. (2011), "A floating platform of concrete for offshore wind turbine", *Renew. Sust. Energ. Rev.*, **3**(6), 063103-063103-063113.

Hywind brochure (2012), Retrieved from http://www.statoil.com/en/TechnologyInnovation/NewEnergy/ RenewablePowerProduction/Offshore/Hywind/Downloads/Hywind_nov_2012.pdf.

Kampf, J. (2009), *Ocean modelling for beginners: using open-source software*, Springer.

Kurian, V., Ng, C. and Liew, M. (2012a), "Experimental investigation on dynamic responses of spar platforms subjected to multi-directional waves", *Proceedings of the Business Engineering and Industrial Applications Colloquium (BEIAC)*, 2012 IEEE.

Kurian, V., Ng, C. and Liew, M. (2012b), "Numerical investigation on dynamic responses of classic spar platforms: Long crested waves vs. short crested waves", *Proceedings of the Humanities, Science and Engineering (CHUSER)*, 2012 IEEE Colloquium on.

Kurian, V.J., Tuhaijan, S.N.A. and Liew, M.S. (2012), "Dynamic responses of spar acted upon by random wave and current", *Proceedings of the Business Engineering and Industrial Applications Colloquium (BEIAC)*, 2012 IEEE.

Leung, D.Y. and Yang, Y. (2012), "Wind energy development and its environmental impact: a review", *Renew. Sust. Energ. Rev.*, **16**(1), 1031-1039.

Moe. (2010), "Floating turbine captures wind energy in deep-water environment", *Weld J.*, **89**(5), 54-58.

Robertson, A.N. and Jonkman, J.M. (2011), *Loads analysis of several offshore floating wind turbine concepts*:

National Renewable Energy Laboratory, US Department of Energy, Office of Energy Efficiency and Renewable Energy.
Sarpkaya, T., Isaacson, M. and Isaacson, M.d.S.Q. (1981), *Mechanics of wave forces on offshore structures* (Vol. 96): Van Nostrand Reinhold Company New York.
Snyder, B. and Kaiser, M. J. (2009), "Ecological and economic cost-benefit analysis of offshore wind energy", *Renew. Energ.*, **34**(6), 1567-1578.
Tavner, P. (2008), "Wind power as a clean-energy contributor", *Energ. Policy*, **36**(12), 4397-4400.
Wang, Y., Yang, J.M., Hu, Z.Q. and Xiao, L.F. (2008), "Theoretical research on hydrodynamics of a geometric spar in frequency-and time-domains", *J. Hydrodynamics, Ser. B*, **20**(1), 30-38.
Wilson, J. F. (2003), *Dynamics of offshore structures*, John Wiley & Sons.

CC